applied sciences

MDPI

Article

Upgrade of the Universal Testing Machine for the Possibilities of Fatigue Tests in a Limited Mode

Róbert Huňady [1,*], Peter Sivák [1], Ingrid Delyová [1], Jozef Bocko [1], Ján Vavro, Jr. [2] and Darina Hroncová [3]

[1] Department of Applied Mechanics and Mechanical Engineering, Faculty of Mechanical Engineering, Technical University of Košice, Letná 9, 042 00 Košice, Slovakia; peter.sivak@tuke.sk (P.S.); ingrid.delyova@tuke.sk (I.D.); jozef.bocko@tuke.sk (J.B.)
[2] Faculty of Industrial Technologies in Púchov, Alexander Dubček University of Trenčín, I. Krasku 941/30, 020 01 Púchov, Slovakia; jan.vavro.jr@fpt.tnuni.sk
[3] Department of Industrial Automation and Mechatronics, Faculty of Mechanical Engineering, Technical University of Košice, Letná 9, 042 00 Košice, Slovakia; darina.hroncova@tuke.sk
* Correspondence: robert.hunady@tuke.sk

Abstract: The object of the upgrade presented in this paper was an older analogue-based universal testing machine preferably designed for tensile testing. The objective of the upgrade was to create a new digitized measurement chain capable of also operating in the mode of simple fatigue tests with cyclic tensile stresses. The upgrade of the equipment mainly included the processes of calibration, creation of related calibration jigs, creation of transformation dependencies and digitization, creation or completion of missing parts of chain-signal conditioning modules, A/D converters, special jigs, etc., as elements of the experimental hardware. The degree of correctness of the calibration and of the transformation dependencies created was verified by regression analysis, and this was verified by simple correlation analysis. The correctness of the proposed modifications, was verified on the basis of the fatigue tests performed for cyclic loading. Thus, it was possible to design, develop and functionally verify a new measurement chain based on an older universal testing machine. Thus, a partially digitized pulsator was created for the possibility of fatigue testing in a technically or functionally limited mode, mainly for educational purposes as a temporary replacement for the order of magnitude more expensive commercially produced test systems.

Keywords: universal testing machines; transducer; cycle fatigue; regression analysis

Citation: Huňady, R.; Sivák, P.; Delyová, I.; Bocko, J.; Vavro, J., Jr.; Hroncová, D. Upgrade of the Universal Testing Machine for the Possibilities of Fatigue Tests in a Limited Mode. *Appl. Sci.* **2024**, *14*, 3973. https://doi.org/10.3390/app14103973

Academic Editors: Przemysław Strzelecki, Michał Stopel and Maciej Kotyk

Received: 30 March 2024
Revised: 29 April 2024
Accepted: 5 May 2024
Published: 7 May 2024

1. Introduction

The processes of investigating the material, often still latent structural properties and behavior of materials are an essential part of the design, assessment, manufacture, operation and maintenance of structural elements and entire structures. The individual properties are then matched by the material characteristics, particularly those of stress, strength, stiffness, deformation, energy, fracture, etc. As a reminder of the whole large range of tests, these are, for example, the examination and testing processes in the field of tensile and compression testing to obtain the basic stress and strain characteristics. Then, there is the whole area of fatigue testing within the analysis of high-cycle but also low-cycle fatigue, transient behaviour, fatigue limit, based on obtaining a number of fatigue curves, such as the Wöhler curve and the Manson–Coffin curve, specifically designed for the area of low-cycle fatigue, the Smith diagram, the Haigh diagram, investigations of processes and crack propagation rates (Paris–Erdogan law), etc. Then, there is the whole field of investigation of materials in terms of its resistance to brittle failure. Either the area of crack arrest philosophy is applied, which includes notch toughness tests (e.g., Charpy type), or full transit curve tests from the area of transient behavior of materials, Nil Ductility Temperature/Transition (NDT) tests (Zero Toughness Temperature), Drop Weight Tear Test (DWTT) tests, etc. Then, there is the whole range of methods for investigating materials

and their resistance to brittle failure based on the philosophy of preventing the initiation and subsequent propagation of fracture. This mainly includes tests for the detection of fracture toughness and fracture behavior of materials, e.g., Stress Intensity Factor, Crack Driving Force, Crack Tip Opening Displacement (CTOD) tests, fracture toughness and generally fracture behavior of materials and their resistance to brittle fracture. These are primarily tests within the framework of linear elastic or elastic–plastic fracture mechanics (LEFM and EPFM). One cannot forget the rather demanding tests for the investigation of materials in the field of elastic–plastic and plastic stresses, conditions and hypotheses of plasticity and Creep deformation as a specific manifestation of plastic deformation and its two basic forms of elastic after-effect and relaxation, and many others. In addition, some tests may be Full-Scale Testing (FST) in nature, which further increases their difficulty [1–3].

The complexity of the processes of analysis of material properties, or in general the behavior of structural materials under different stress conditions and the influence of other adverse factors or material degradation factors can be documented by the example of obtaining a full Wöhler curve according to Figure 1 [1]. This is composed of a number of partial fatigue curves obtained by appropriate fatigue tests. In analyses of a similar nature, attention is almost always directed only to the limiting failure situation of the specimen, i.e., directly to the fatigue curve line for a particular combination of stress spread $\Delta\sigma$ or stress amplitude σ_a on the number of cycles N. A less frequently studied issue, but an important area for understanding the behavior of materials, is also the investigation of the changes in the properties, the state of the material and the degree of accumulation of its fatigue damage at a certain stress level $\Delta\sigma$ completely from the beginning of its stressing, i.e., for $N = 0$ up to the limiting number of cycles $N_{\Delta\sigma}$ of the failure of the specimen by the processes. The individual phenomena, states and the relationships between them are also important. For example, in Figure 1, these processes are represented by several stages of fatigue failure accumulation under stress below the dynamic yield strength, separated by lines 1 to 7.

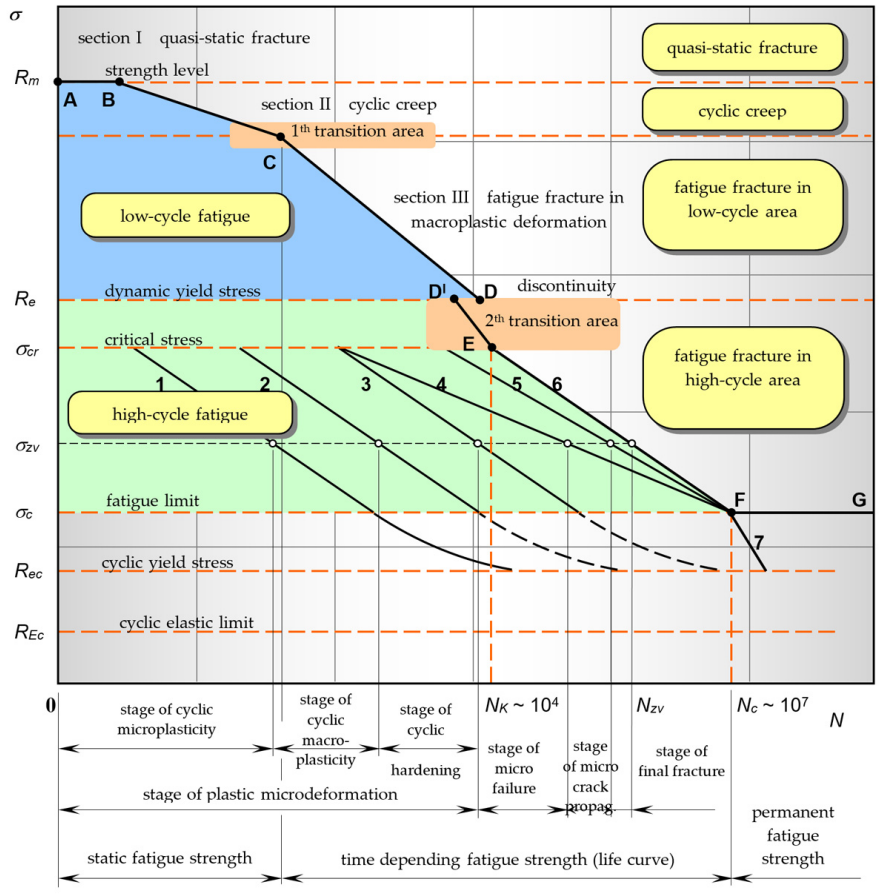

Figure 1. Schematic of the full Wöhler curve.

However, all these material testing processes are characterized by their high demand on time, technical and software resources and are therefore economically and logistically demanding. They are also demanding in terms of implementation procedures, methodology of acquisition, processing and, most importantly, professionally and scientifically acceptable interpretation and their integration into the already existing database of knowledge and information, verification of existing, or creation of new hypotheses about the nature of certain physical processes and also the relationship between them. Such processes, however, require modern sophisticated, nowadays fully computer supported and therefore digitized testing techniques and equipment.

2. Reasons for Applying the Upgrade

In technical engineering practice, there are situations, caused by various, e.g., technical, economic, operational and other factors, where the relevant test equipment or facilities are not available, or that morally older but still fully functional equipment is available. It is now a question or a dilemma whether there is some possibility of upgrading, modernization, transformation, redesign, associated digitization and computer-aided experimentation, etc. The final form and possibilities of the facility must be taken into account, so that any such modifications are also technically possible, efficient and economically acceptable. For such modified equipment with added functionality, there is then a tendency to require the ability to maintain the nature, stability, level and intensity of the test quantities. These are mainly force, stress, strain, temperature, frequency, etc., quantities as characteristic parameters of the equipment and the test methodologies and procedures linked to them.

The issue of implementing such upgrades is particularly relevant in the field of education and training, or for small companies and other entities. These are typical examples of entities for which the expenditure of larger funds is particularly sensitive, especially in view of the limited financing possibilities. In such a case, there is an opportunity to use older existing equipment as an albeit temporary replacement for admittedly new and advanced test systems, but also orders of magnitude more expensive compared to the cost of a less demanding upgrade. It is then a question of choosing the method of this upgrade, i.e., whether it should be a modernization, refurbishment, redesign, digitization, etc. At the same time, the degree or extent of this upgrade must be chosen in light of the available funding options.

Obviously, the design and implementation of any modifications to any older test device will always present necessary emergent trade-offs. These will be linked to an assessment of all relevant factors, mainly of a time, technical and economic nature, with regard to the resulting level and type of functionality and the parameters achieved by the equipment so upgraded.

3. Examples of Ways and Reasons for Upgrading in Technical Practice

From the wide range of information available on the methods and reasons for upgrading test machines or entire measurement chains and test methods in technical engineering practice, several examples can be given from different fields of application.

McAlorum et al. in [4] presents a description and a certain solution to the practice situation, when before deployment of components in industrial applications it is advisable to perform mechanical fatigue tests of the materials used and of the whole prototype structures. However, such fatigue tests often require continuous long-term application of a suitable handling and clamping fixture. However, this can present a problem in terms of outsourcing the testing and can also be limiting in terms of the ability to adapt quickly and easily to a particular type of test. This paper presents the design and feasibility of a simple low-cost, adaptable jig designed for bending fatigue testing of structural elements. The jig was designed and evaluated using FEM and later on real long-term experiments to verify the longevity of the jig. Compared to outsourcing, this design is cost-effective, according to the authors, if longer-term tests are planned at the level of more than 373 h of testing. An assembly using the test machine and the proposed jig will allow for continuous

long-term fatigue testing while allowing for multiple customization options. The options, among others, consist in the ability to choose the method of fatigue loading of the beam in the mode of three-point or four-point bending, with the choice of the level of minimum (as compressive) and maximum (as tensile) loading force and loading speed.

A remarkable example according to [5] was even not only the development but also the actual production of a simple experimental device based on commercially available components such as an electric drive motor or digital speed sensor. A custom clamping frame with integrated spring load system was also developed and manufactured. The testing machine was developed for the purpose of rotational bending tests based on the R R. Moore principle for educational or less demanding commercial applications. It was designed and implemented at a fraction of the cost required to purchase or procure a commercially manufactured product.

Jimenez in [6] presents a description of the redesign and automation of a machine for fatigue testing in rotational bending by applying knowledge and principles from mechatronics. The publication presents examples of the final design and how to apply the LabView graphical programming tool in the development of the control interface and in the simulation of the tests.

The contribution [7] brings a study of low-cycle fatigue analysis using miniature specimens under high temperature conditions and considering the effects of surface roughness and residual stress. These miniature specimens with a non-standard test cross-section diameter of 1 mm were taken from the failed portions of standard size specimens. Based on the verification tests, the results were found to be in relative agreement with those obtained on the large 6.5 mm diameter specimens. By shrinking the test specimens, these efforts bring about a streamlining of testing and methodology, material savings and thus modernization of test equipment and entire measurement chains by miniaturizing them. A presentation of similar efforts and activities can be found, e.g., in the works [8,9].

Pach et al. in [10] discusses the problem of design and implementation of a relatively simple test device for fatigue testing of fiber-reinforced polymer (FRP) composites. The proposed device allowed to take into account several important parameters such as fiber/matrix ratio, fiber orientation, and order of fiber deposition. At the same time, it allowed the tests to be carried out at low frequencies in order to avoid temperature rise in the polymer matrix, which could degrade the mechanical properties of the composite. The equipment also allowed multiple specimens to be tested simultaneously, thus reducing the time required to obtain the required complete set of fatigue characteristics. According to its designers, the equipment thus designed represents a reasonable cost alternative compared to conventional but far more expensive industrially manufactured servo-hydraulic testing machines.

Another example of upgrading legacy test machine infrastructure according to [11] was the engineering design and implementation of an information system based on the Internet of Things (IoT). It was designed to remotely, collect, store and process information on the number of mechanical cycles performed for a group of legacy existing fatigue testing machines in the automotive industry for component manufacturing. Important was the possibility of automatic detection of the end of fatigue tests, thus achieving a more efficient utilization of the testing machines, according to the authors' data at a level of more than 25%. The electromechanical cycle count sensors were replaced by electronic sensor modules in the role of so-called clients with a newly developed Ethernet interface, working with a free Linux server and a web application framework. The results achieved were comparable to the manual data collection method. This was a relatively very affordable upgrade of older test machines without the need to buy expensive industrial communication systems.

The work [12] addresses the issue of high cost and how this can be addressed, where the range of cost for a typical fatigue testing training device is between USD 10,500 and USD 32,500. These devices are essentially adaptations of the R. R. Moore methodology testing machines with a price level of even more than 150,000 USD. Therefore, the author is

looking at ways to produce affordable and fully functional versions of the equipment with appropriate test methodologies that will also provide reliable results.

In contribution [13], a description of a newly developed simple test device for testing the dynamics of fatigue crack propagation is given. The apparatus, capable of high frequencies up to 4 kHz, allows to load the test specimen with inertial forces up to 2.9 kN, with their arbitrary course, at a value of 100 kg payload. The base of the fatigue vibration machine is a sliding table mounted on a granite base, providing a solid base for stability of the set parameters. An electromagnetic vibration unit from Ling Dynamic Systems, model V722, with a clutch that also allows for angular deflection, was chosen for the drive. According to the author's own evaluation, such a device can bring significant cost reductions compared to other comparable test rigs, e.g., of the Wiercigroch design.

In [14] by Ogawa et al., an example of a test machine upgrade is given with the design of a test fixture capable of performing high-cycle multiaxial fatigue tests. The newly developed test chain allows to combine bending and torsional stresses and to perform fatigue tests at high frequency up to 50 Hz. The loading itself can be proportional and non-proportional, where the direction of the principle stress can be varied during the cycle. Proportional loading here means cyclic bending loading and non-proportional loading is cyclic loading combining bending and reverse torsional loading. Strain gauge sensing of the quantities is part of this measurement chain and the digitization is realized by the application of an electronic control unit and an I/O A/D PC card.

Upgrade processes of a similar device, which is also the subject of this paper, can be implemented by modifications, e.g., according to [15]. Its essence was the extension of the device with a multifunctional measuring card PCA 1408 (ADICOM) with Control Panel application software, strain gauge control panel UPM 60 from HBM and a digital caliper. A major contribution to the upgrade of the entire device was its digitization. This is because the application and control test software allowed customization for the user's needs. It also offered predefined basic cross-section shapes. The result was then an increase in comfort but also in the speed of the experiment. It was also possible to make repeated measurements of a certain dimension and from such measurements to determine the average values entering into further measurements or analyses. The developed software also included an evaluation part for the basic types of mechanical tests of the material. The data thus measured could be directly processed and used to determine the material characteristics of the test specimens. The measured data could also be further exported and processed by third-party software. This made the equipment comparable to new but much more expensive testing systems in its time.

This was just a brief overview of not only the proposed, but also actually implemented and fully functional solutions for upgrading, digitalization, modernization, redesign and modifications for further possibilities of using older, but still fully functional and operational test machines. In these cases, there has been a sort of reincarnation of older equipment that, although fully functional but already morally obsolete in its original form, would not stand up to the current advanced but also far more expensive equipment. In some cases, it has also involved the development of new equipment with test methodologies that minimize operating costs, time, increase equipment flexibility, etc. The description and characterization of other remarkable possibilities can be found in a number of other works, such as [16–18]. All these mentioned cases of legacy equipment upgrades have provided evidence of the relevance, meaningfulness and even some timeliness of such activities and have also contributed in no small measure, albeit only on a motivational and suggestion basis, to the idea and implementation of the equipment upgrade described in this paper.

4. The Nature and Objectives of the Testing Machine Upgrade

The object of the upgrade mentioned in this paper was an older HECKERT FPZ 100/1 universal testing machine (VEB Thüringer Industriewerk, Rauenstein, Germany), described in more detail in the next chapter. The objective of the upgrade was to create a new digitized measurement chain capable of also operating in the mode of simple fatigue tests with cyclic

loading. The upgrade of the equipment mainly included the processes of calibration and creation of related calibration jigs, creation of transformation dependencies, digitization, assembly of the new measurement chain and creation of its missing parts as elements of the experimental hardware. The accuracy rate of the calibration and the created transformation dependencies was verified by regression analysis, and the latter was validated by simple correlation analysis. The correctness of the proposed modifications, the degree and quality of the functional verification after the applied modifications to meet the new requirements was finally verified on the basis of the fatigue tests performed for cyclic loading but with the implementation in a limited mode.

The integral parts of the HECKERT FPZ 100/1 testing machine upgrade, discussed and described in this paper are mainly:

- Completion of measurement chain;
- Calibration of transducers, creation of transformation dependencies and regression analyses;
- Perform of verification experimental low-cycle fatigue test measurements;
- Assessment of limitations of the newly established measurement chain after the upgrade of the FZP 100/1;
- Overall evaluation of the upgrade, modernization and redesign of the FZP 100/1 test facility;
- Considerations for further upgrade of the FZP 100/1.

5. FPZ 100/1 Test Equipment

The HECKERT FPZ 100/1 test device, which is the object of the upgrade, is a universal testing machine with a maximum load of 100 kN with a typical design according to Figure 2. The force is exerted by a mechanical transmission with an electric drive. The drive train includes a thyristor rectifier with a control device, a DC motor and a four-speed control gearbox, guaranteeing a large range of test speeds with high stability. The measurement of load force and elongation is realized by electrical sensors of physical quantities-transducers. These have the character of a dynamometer for measuring forces and an extensometer for measuring absolute elongation. There is a set of interchangeable force transducers (dynamometers) with force levels of 40 N, 400 N, 10 kN and 100 kN for the tension modes and one 100 kN force transducer for the pressure mode. The measurement of tensile and pressure forces, respectively, is performed by an interchangeable electronic transducer using the principle of inductive path measurement. The measured values are displayed analogue on a circular scale and can be additionally registered by means of a registration device or peripheral devices can be connected. Changes in length may be measured by deployable extensometers with a transducer character in the range from 50 μm to 50 mm, or by resistive sensors, which sense the traverse displacement in the range from 10 mm to 935 mm. The measured values are displayed on a flat scale and can be recorded on a recording device, again with peripheral devices [19].

On the left side at the top is the main control unit, at the bottom is the electromechanical drive. On the right side is the load frame itself with two working areas separated by a movable traverse on which the clamping and force measuring elements are installed. The work space at the top is for tension mode tests and the lower work space is for compression mode tests. Clamping and force measurement elements are then installed in the upper bracket in the upper section and the lower bracket in the lower section, paired with the clamping and force measurement elements of the movable bracket. When loading the test specimen in both tension and compression, the traverse always moves downwards. Its maximum stroke is 935 mm. An integrated recording device allows changes in load and specimen elongation to be recorded in force vs. strain, force vs. time and strain vs. time diagrams.

Figure 2. Typical form of the HECKERT FPZ 100/1 universal testing machine.

In the case of the FPZ 100/1 device, it is not a pulsator with an electrohydraulic drive, directly designed for fatigue tests, but a universal testing machine on an electromechanical basis. Therefore, it is preferably intended for static tensile or compression tests and thus for obtaining strength and deformation characteristics. The possibilities of the pulsation function as a pulsator, i.e., for cyclic loading, is only supplementary, with limited possibilities. These are mainly related to the possibility of loading either only in tension or only in compression mode, i.e., without the possibility of simultaneous alternating tension and compression loading for an alternately symmetrical or asymmetrical cycle. There are two separate working spaces for tension and compression tests. Another limiting factor for the functionality of the pulsator is the loading frequency. This is listed in the datasheet of the device as the so-called switchable frequency, continuously variable up to the maximum value at the level of only 0.1 Hz. The speed of movement of the clamping jaws is given in the range of 0.00035–10 mm/s.

This device, based on a 1980s design, is in its basic configuration with purely analogue drive, control and indication of variables. A 10 V, 5 mA analogue output indication voltage signal is provided for peripheral connection, storage and further data processing. The AC component of the analogue signal $U_{\Delta l}$ corresponds to the measured deformation and the DC component of the analogue signal U_F corresponds to the measured load force.

The device also includes a number of other accessories and interchangeable jigs. These not only allow the testing of classical engineering construction materials based on ferrous and non-ferrous metals and their alloys, but due to the large range of movement speeds and interchangeable clamping elements, this equipment is also suitable for the measurement of samples made of non-metallic materials, e.g., plastic, rubber, wood, paper, textiles, composites and even biological materials.

6. Creation of a Digitized Measurement Chain

One of the first essential steps for upgrading and digitizing the test equipment was to create a complete measurement chain. The main elements of this chain were the FPZ 100/1 device itself with its TD1 and TD2 transducers as extensometers and the PC assembly. These separate devices had to be connected by another important hardware component. This was the MF 624 multifunction I/O card (Humusoft, Prague, Czech Republic). This card is, among other things, suitable for connecting sensors and transducers and for measuring DC voltages. It operates at input voltages in the range of ±10 V. It is therefore suitable for connection to the 10 V output of the FPZ 100/1. This connection was implemented

via two analogue inputs with A/D converter with a conversion time for the two inputs of 1.9 µs. The PC setup used was also equipped with a cooperating software package. This software package included MS Excel spreadsheet as part of the Microsoft Office 2013 Professional Plus environment, Matlab 9.0 software with Simulink and Real Time Toolbox add-on modules. The Real Time Toolbox allowed the MF 624 card to efficiently use all the capabilities of the MF 624 card for real-time measurements. Then, in the environment of MS Excel and Matlab software, most of the evaluations of the measured data, regression analyses and their graphical visualization were performed.

One of the problems solved was the problem of signal incompatibility between the 10 V analogue outputs of the FPZ 100/1 test machine and the inputs of the MF 624 multifunction I/O card. Since the MF 624 I/O card is only capable of measuring DC voltages and the $U_{\Delta l}$ signal attributed to the change in length Δl had the shape of an AC voltage, it was necessary to make a correction of the signal to DC. A Signal Conditioning Module SCM as a conditioning device was designed and fabricated according to the schematic in Figure 3. This figure also shows its interfacing with the FPZ 100/1 machine and the MF 624 I/O card interfaced with the PC. The bridge Graetz rectifier wiring (Module I) was applied. Subsequently, high-frequency noise was removed from the signal using a capacitor filter (Module II). The voltage signal U_F attributable to the force was already DC at the output of the test machine, thus no rectification was necessary. Finally, both signals were still adjusted in the decoupling amplifiers (Module III and IV).

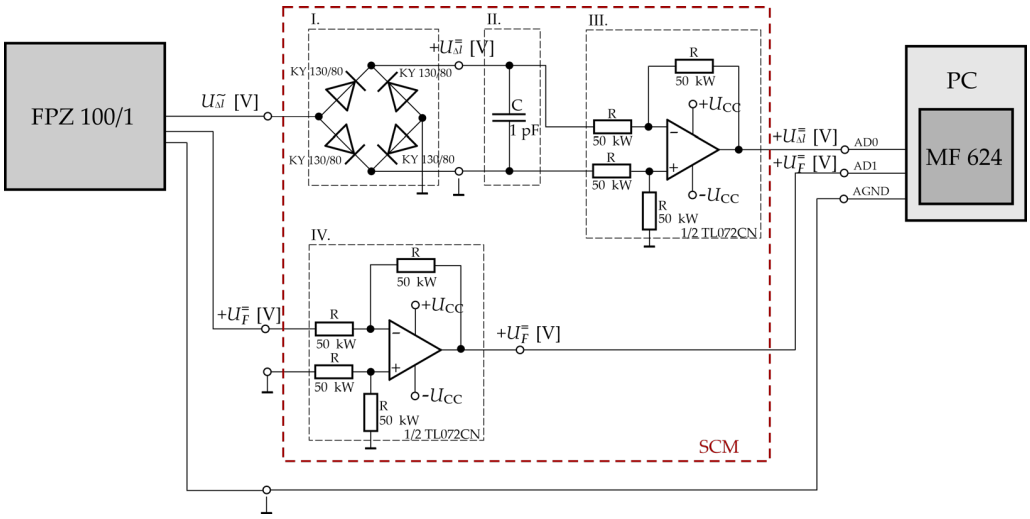

Figure 3. Electrical diagram of the Signal Conditioning Module SCM and its interfacing with the FPZ 100/1 machine and the MF624 I/O card in the PC.

7. Test Specimens and Test Materials

For the calibration of the transducer extensometers TD1 and TD2 and for the low-cycle fatigue measurement process itself, several test specimens made in two shape modifications from two different steel materials were used.

All specimens used in the TD1 extensometer measurements were made of material 12 010 according to STN or ČSN (Slovak or Czech technical standard) 41 2010. Its equivalents are steels with the designation ISO C10, DIN C10, Ck 10 1.0301, e.g., according to [3]. This is a carbon steel for cementing intended for the production of pins and shafts. Material characteristics such as yield strength σ_y and ultimate strength σ_u (or f_y and f_u according to the Eurocode 3 standards) are given in the available sources in a wide range of 165–345 MPa for σ_y and 290 to 845 MPa for σ_u. The specific value depends on several factors such as the type and degree of heat treatment and material thickness. Based on the measurements of the applied steel modification, a tensile diagram F-Δl was found according to Figure 4a with approximate values of 318 MPa for σ_y and 454 MPa for σ_u.

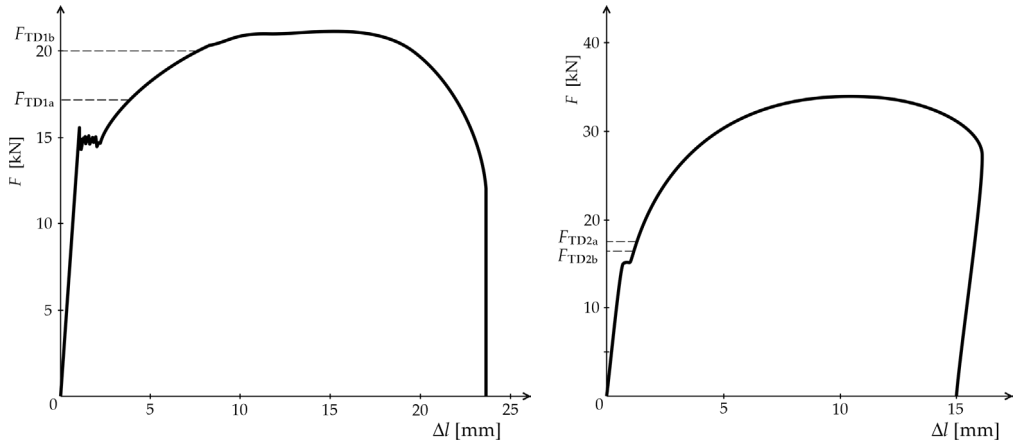

Figure 4. Tensile diagrams in *F*-Δ*l* system for test specimens with actual diameter 7.75 mm for materials: (**a**) 12 010; (**b**) 14 109.3.

All specimens used in the TD2 extensometer measurements were made of material 14 109.3 according to STN or ČSN 41 4109. Its equivalents are steels with the designation ISO Type 1-0 683/17-73, EURO 100Cr6 EN94-73 or DIN 100Cr6 17230-80. This is a chromium steel for rolling bearings in the soft annealed condition. Material characteristics such as yield strength σ_y and ultimate strength σ_u are quoted in the available sources in the range 423 to 468 MPa for σ_y and 628 to 765 MPa for σ_u. The specific value again depends on several factors such as the type and degree of heat treatment and material thickness. Based on the measurements of the applied steel modification, a tensile diagram *F*-Δ*l* was found according to Figure 4b with approximate values of 317 MPa for σ_y and 699 MPa for σ_u. For the calibration of the TD2 transducer, specimens of this material with an actual diameter of 9.61 mm were further hardened and tempered by hardening and tempering for the purpose of calibrating the TD2 transducer to expand the elastic deformation region.

The shape and dimensions of the test specimens of material 12 010 and of material 14 109.3 used in the calibration and fatigue tests are shown in Figure 5a,b. These were specimens with a cylindrical working part with a circular cross section. The circular cross-section diameters of 8 mm and 10 mm shown are nominal only. The actual diameter values as a result of surface treatments dropped to 7.75 mm and 9.61 mm. The tensile diagrams in Figure 4 were obtained for the 7.75 mm diameter specimens. The force levels F_{TD1a}, F_{TD1b}, F_{TD2a} and F_{TD2b} indicated in the tensile diagrams, and their corresponding normal stresses σ were later used in the low-cycle fatigue analysis. The use of test specimens of several shape, size, material modifications and structural states was related precisely to their different physical availability or unavailability during these measurements.

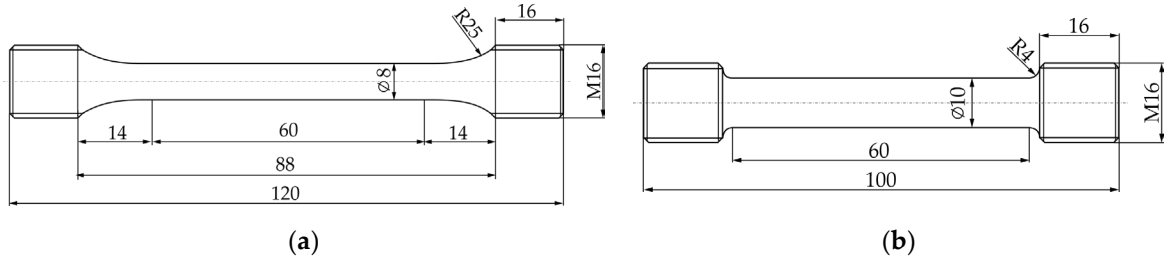

Figure 5. Shapes and dimensions of test specimens of materials 12 010 and 14 109.3 with nominal diameter: (**a**) 8 mm; (**b**) 10 mm.

8. TD1 and TD2 Transducer Calibration Processes

From the extensive accessories of the FPZ 100/1 machine, two types of transducers TD1 and TD2 (Figure 6) were used as extensometers for the purpose of upgrading the measurement chain and for calibration, experimentation and analysis of low-cycle fatigue under cyclic loading for the measurement of the absolute elongation Δl. These are transducers based on inductive transducers in two different sensitivity levels. The transducer type in the TD1 design has for each Scale Factory SF 10:1, 20:1 and 40:1 corresponding measurement ranges of absolute elongations Δl of 10–50, 5–25 and 2.5–12.5 mm, respectively, with a total corresponding range of relative elongations of $1.25 \cdot 10^{-2}$ to 2.5%, for measured lengths l_0 ranging from 20 to 200 mm. The transducer type in the TD2 version has for each Scale Factory SF 500:1, 1000:1 and 2000:1 the corresponding measurement ranges of absolute elongations Δl of 0.2–1.0, 0.1–0.5 and 0.05–0.25 mm, respectively, with a total corresponding range of relative elongations of $1.0 \cdot 10^{-3}$ to $5.0 \cdot 10^{-2}$%, for measured lengths l_0 in the gradations 20, 30, 40 and 50 mm.

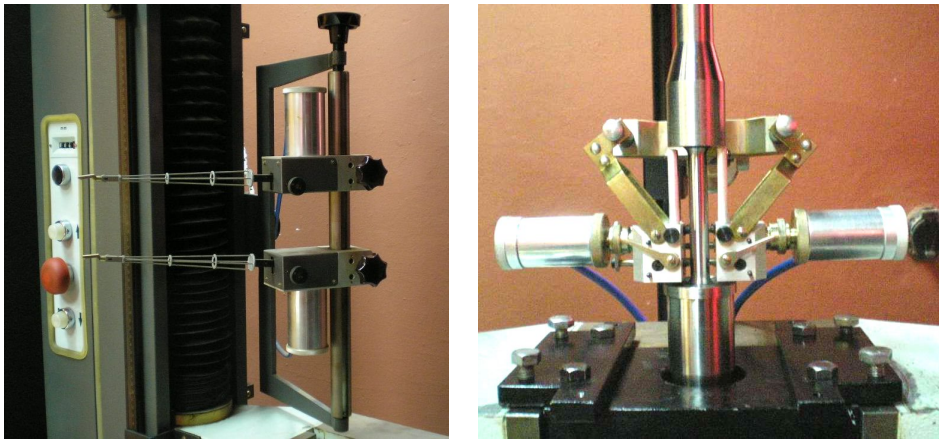

(**a**) (**b**)

Figure 6. Transducers TD1 and TD2 for measuring absolute elongations Δl based on inductive transducers, used in calibration and low-cycle fatigue analysis processes: (**a**) TD1 in the free unapplied position; (**b**) TD2 in the calibration mode.

In order to verify the functionality of the transducers and the correctness of the data measured by them and to verify the functionality of the 10 V output of the FPZ 100/1 machine before the actual fatigue analysis processes, it was necessary to subject these transducers to calibration processes.

8.1. TD1 Transducer Calibration Process

For the calibration of the TD1 transducer, a specially developed single-purpose test jig according to Figure 7a with contact surfaces for clamping the TD1 transducer arms was clamped in the clamping jaws of the FPZ 100/1 machine instead of the test specimen. A total of two LARM MSL30.152 PA measurement probes [20] were integrated into this jig. The probes are used for precise measurement of length coordinates in the measurement range of 30 mm. The LARM measuring probe is equipped with a return spring with a defined maximum pressure of 1 N. The supply voltage of the probe is +5 V and its measuring step is 5 µm. The optical information about the position of the measuring rod is transformed by electronic circuits into electrical pulses of incremental type. The obtained signal was processed by Matlab software. The test fixture together with the LARM probes and the TD1 transducer is shown in Figure 7b. The electrical diagram of the interconnection of the FPZ 100/1 machine, the MF624 I/O card, the PC, the Signal Conditioning Module SCM and the pair of LARM MSL30.152 PA measurement probes for the purpose of calibration of the TD1

transducer is shown in Figure 8. The output of the LARM probes was fed to the MF624 I/O card via its incremental sensor inputs during the measurement.

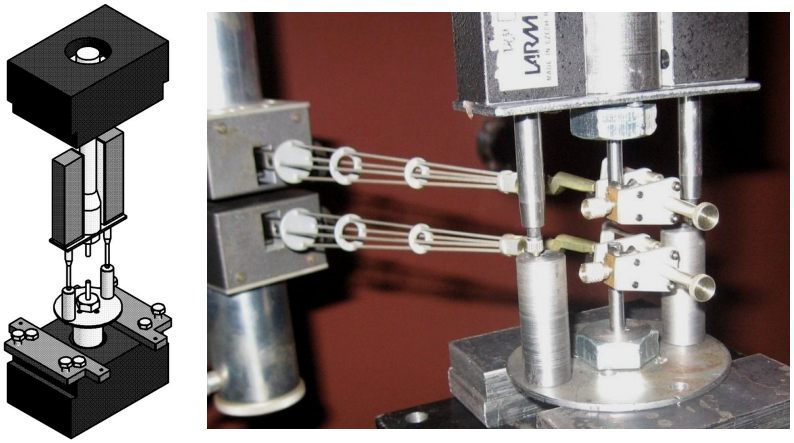

(**a**) (**b**)

Figure 7. (**a**) Test jig with integrated LARM MSL30 measurement probes for the TD1 transducer calibration process; (**b**) test fixture clamped in the jaws of the FPZ 100/1 in the TD1 transducer calibration process.

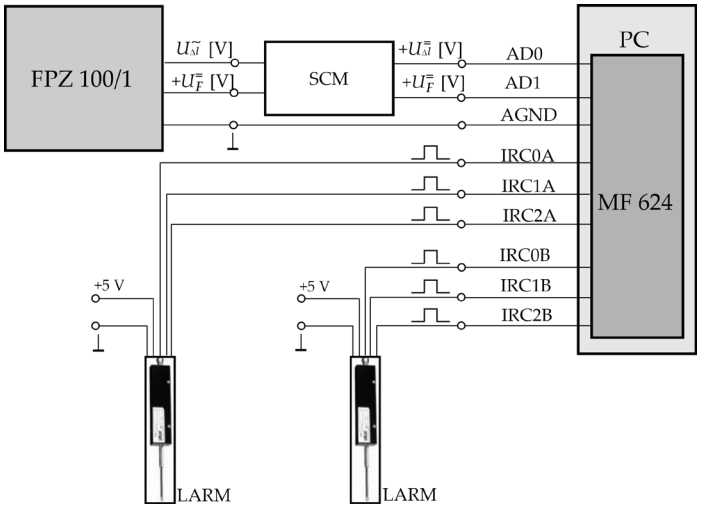

Figure 8. Electrical diagram of the interconnection of the FPZ 100/1 machine, I/O card MF624, PC, Signal Conditioning Module SCM and a pair of LARM MSL30.152 PA measurement probes for the calibration of the TD1 transducer.

The correct function of the extensometer was verified by several measurements on two measured lengths of the fictitious measurement base l_0 20 mm and 100 mm and at all available Scale Factors SF of 10:1, 20:1 and 40:1. During the calibration, the elongation values Δl [mm] from the FPZ 100/1 machine indicator and the related length change values in the electrical voltage variable $U_{\Delta l}$ [V] simultaneously recorded by the I/O card in the PC and the elongation or length change values Δl [mm] obtained from the LARM MSL30 sensors were recorded. To create the calibration dependencies and curves, the Δl values obtained from the FPZ 100/1 machine indicator had to be converted to units of [mm] mm using the appropriate Scale Factors SF. The values so adjusted were plotted on a graph versus the values of the change in length Δl [mm] obtained from the LARM MSL30 sensors. Detailed calibration results are given in a separate chapter.

8.2. Transducer TD2 Calibration Process

During the implementation of the TD2 transducer calibration process, there were several issues that needed to be resolved. The first was that due to the nature of the experiment and the dimensions of the TD2 transducer, it was not possible to use the calibration methodology as for TD1, i.e., using a test jig with integrated LARM MSL30 measurement probes. This problem was solved by using elongation values calculated from the values of the loading forces taken from the FPZ 100/1 machine indicator. However, for this method of measurement, physical test specimens had to be clamped in the clamping jaws of the FPZ 100/1 machine, unlike the use of virtual specimens in the case of the TD2 calibration.

The second problem was related to these test specimens or to the unsatisfactory deformation characteristics of the materials of these specimens. For calibration purposes, several test specimens with shapes and dimensions according to Figure 5b of material 14 109.3 were applied. The tensile diagram for a diameter of 7.75 mm according to Figure 4b or for a diameter of 9.61 mm according to Figure 9 of curve (a) resulted in a yield strength value σ_y of 317 MPa. Also considering the planned experimental measurements in the elastic–plastic or plastic deformation area, where the deformations could far exceed the deformations corresponding to a stress value of 317 MPa, the yield strength value for these purposes was very low. To increase the elastic deformation range, the specimen was primarily subjected to strain hardening by plastic deformation and secondarily to hardening and tempering. For completeness, the process parameters are also given: preheating at 600 °C for 10 min, heating at 830 °C for 15 min and finally tempering at 410 °C for 2 h.

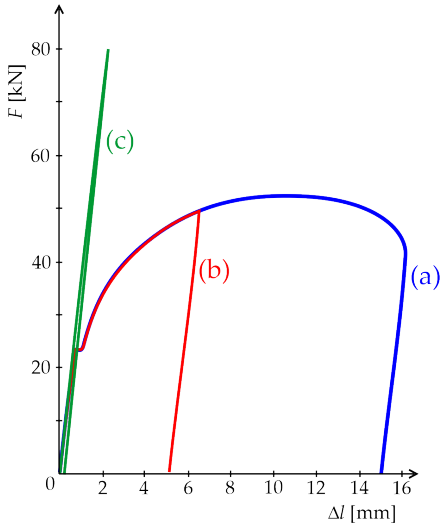

Figure 9. Tensile diagram of a 9.61 mm diameter specimen of 14 109.3 (**a**) in the original structural state without change in mechanical properties and after change in mechanical properties in the new structural state by expansion of the elastic deformation region as a result of (**b**) strain hardening and (**c**) heat treatment of the specimen by hardening and tempering.

Figure 9 shows the tensile diagrams of 9.61 mm diameter specimens of 14 109.3 material in three structural states. Curve (a) represents the material in the original structural state with no change in mechanical properties. Curves (b) and (c) represent the specimen after the change in mechanical properties in the new structural states by expansion of the elastic deformation region. Curve (b) is the result of strain hardening by plastic deformation and curve (c) is the result of heat treatment of the specimen by hardening and tempering. These modifications gradually extended the elastic deformation area first to a force of F = 50 kN for method (b) and then to a force of F = 80 kN for method (c). For this value, a sufficiently large margin of the elastic deformation range was then already established.

The measurement was performed at the maximum possible measured length l_0 = 50 mm, identical to the maximum length of the measuring base of the TD2 transducer. Of the available Scale Factor SF values for the TD2, the most sensitive one of 2000:1 was used. To verify the correctness of the results, this measurement was performed three times. Since no significant differences between the measured data were found, it was possible to proceed to their evaluation. The length change values read from the Δl indicator of the FPZ 100/1 machine were, as in the case of the TD1 calibration, corrected by the appropriate Scale factor SF. Since it was not possible to use the LARM MSL30 probes for the accurate measurement of the compared direct elongation Δl on the clamping jaw side, the analytically calculated value of the measured length change Δl was used as the reference value for the construction of the calibration curves. This was obtained from the actual value of the loading force F read from the force indicator on the FPZ 100/1 testing machine and its adjustment using the Hooke's law relations for tension according to $\Delta l = 4\,F{\cdot}l_0/(E{\cdot}d{\cdot}\pi{\cdot}^2)$. The following numerical values were applied: the length of the measuring base l_0 = 50 mm, the Young's modulus of elasticity in tension for steel $E = 2.05{\cdot}10^5$ MPa and the diameter of the circular cross-section d = 9.61 mm.

For calibration, the TD2 transducer was applied to the test specimen according to Figure 6b, and the electrical wiring scheme was applied according to Figure 10. Figure 11a shows the calibration dependence curve obtained from the data measured in the test with a measured length of l_0 = 100 mm and a Scale Factor SF of 40:1. Figure 11b shows the calibration dependence (curve) obtained from the data measured in a test with a real specimen with a measured length of l_0 = 50 mm and a Scale Factor SF of 2000:1.

Detailed calibration results are given in a separate chapter.

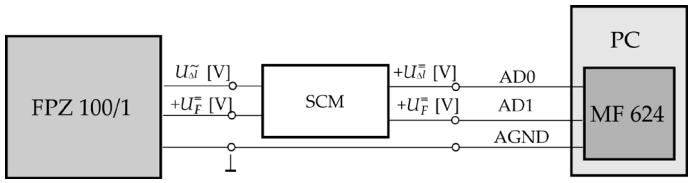

Figure 10. Electrical diagram of the interconnection of the FPZ 100/1, I/O card MF624, PC and Signal Conditioning Module SCM for the calibration of the TD2 transducer.

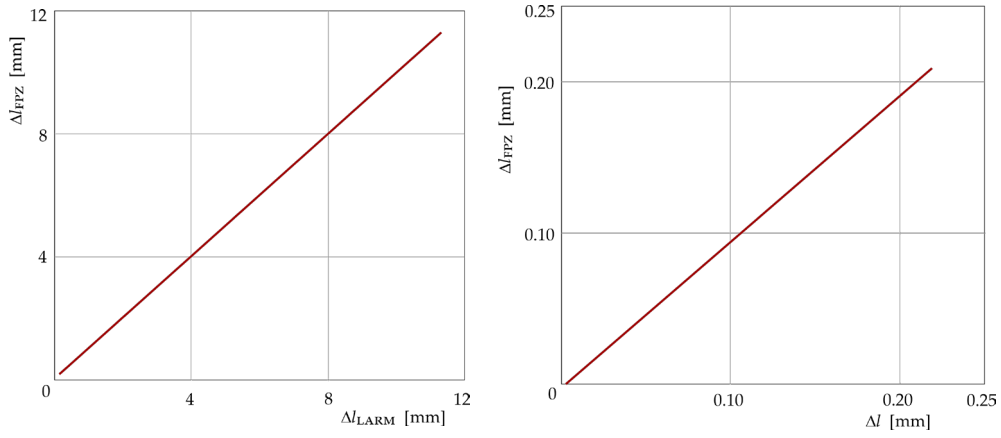

(**a**) (**b**)

Figure 11. Calibration dependence (curve) obtained from the data measured during the calibration test: (**a**) transducer TD1 with fictitious measured length l_0 = 100 mm and Scale factor SF 40:1; (**b**) transducer TD2 with real measured length l_0 = 50 mm and Scale factor SF 2000:1.

8.3. Conversion (Transformation) Dependencies for the 10 V Output

The values obtained from the 10 V electrical output of the FPZ 100/1 were in the form of voltage signals U_F and $U_{\Delta l}$ [V]. Because of this, it was necessary to transform these

signals into suitable final outputs, i.e., [kN] for the force F and [mm] for the change in length Δl, and to create the appropriate transformation dependencies. Figure 12 shows the calibration curves of the transformation dependence Δl vs. $U_{\Delta l}$ of the TD1 transducer always with load and unload branches for three Scale Factor SF values of 10:1, 20:1 and 40:1.

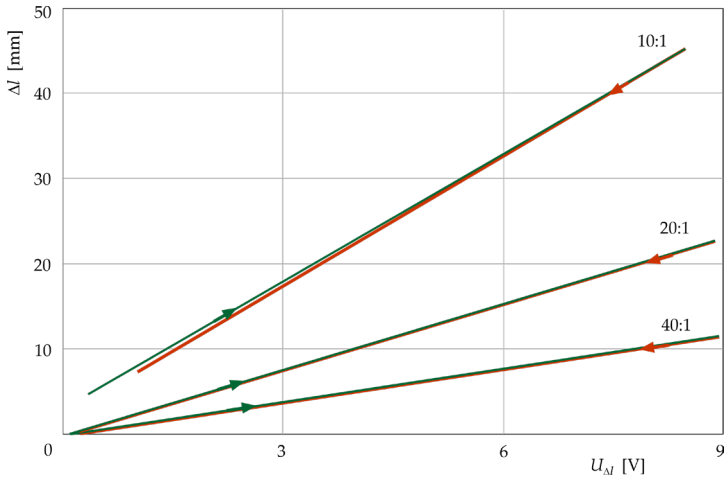

Figure 12. Calibration curves of the transformation dependence Δl vs. $U_{\Delta l}$ of the TD1 transducer always with load (green line) and unload (red line) branches for three values of Scale Factor SF 10:1, 20:1 and 40:1.

Figure 13a shows the calibration curves of the transformation dependence always with load and unload branch for F_{FPZ} vs. U_F. Figure 13b shows the calibration curves of the transformation dependence always with load and unload branch for Δl vs. $U_{\Delta l}$ transducer TD2 for Scale Factor SF 500:1. Detailed calibration results are given in a separate chapter.

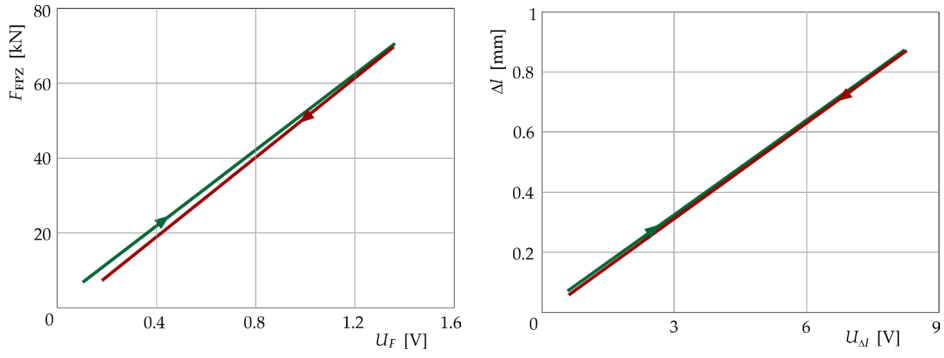

(**a**) (**b**)

Figure 13. Calibration curves always with load (green line) and unload (red line) branches: (**a**) transformation dependence of F_{FPZ} vs. U_F; (**b**) transformation dependence of Δl vs. $U_{\Delta l}$ of transducer TD2 for Scale Factor SF 500:1.

8.4. Summary Results of Calibration Processes

In all cases of calibration, a regression dependence was created with a linear regression model according to $y = a \cdot x + b$ with regression parameters a and b, e.g., according to [21]. All the essential information of the calibration process and regression analysis is given in Table 1. For each transducer TD1 or TD2, the value of the Scale Factor SF, the loading mode (loading/unloading), the type of variable (quantity) for the horizontal x-axis and the functionally related quantity for the vertical y-axis are given, with the corresponding physical units. The parameters a and b *of* the linear regression dependence are given below. The degree of correlation of the proposed regression model with the statistical data set

was verified by the dimensionless coefficient of determination R^2. The physical unit [**] of parameter b corresponds to the physical unit of the quantity y, and the physical unit [*] of parameter a corresponds to the physical unit of the proportion of the quantities y/x. The data marked with x are not specified.

The regression analysis was performed in the Matlab and MS Excel environment as a part of Microsoft Office.

Table 1. Parameters of the calibration process, regression analysis and other related information.

Transducer	Scale Factor	Loading Mode	x	y	a [*]	b [**]	R^2 [-]	Hysteresis	Figure No.
TD1	40:1	loading	Δl_{LARM} [mm]	Δl_{FPZ} [mm]	0.9957	0.0450	1.0000	x	Figure 11a
TD2	2000:1	loading	Δl [mm]	Δl_{FPZ} [mm]	0.9558	−0.0008	0.9986	x	Figure 11b
TD1	10:1	loading	$U_{\Delta l}$ [V]	Δl [mm]	4.9813	2.9473	0.9998		Figure 12
	10:1	unloading	$U_{\Delta l}$ [V]	Δl [mm]	5.1021	2.2094	1.0000	from	Figure 12
TD1	20:1	loading	$U_{\Delta l}$ [V]	Δl [mm]	2.5392	−0.1658	0.9999		Figure 12
	20:1	unloading	$U_{\Delta l}$ [V]	Δl [mm]	2.5463	−0.2930	1.0000	from	Figure 12
TD1	40:1	loading	$U_{\Delta l}$ [V]	Δl [mm]	1.2705	−0.1470	1.0000		Figure 12
	40:1	unloading	$U_{\Delta l}$ [V]	Δl [mm]	1.2698	−0.1590	1.0000	from	Figure 12
x	x	loading	U_F [V]	F_{FPZ} [kN]	50.8390	1.2317	0.9970		Figure 13a
	x	unloading	U_F [V]	F_{FPZ} [kN]	51.2880	−1.3665	0.9975	low	Figure 13a
TD2	500:1	loading	$U_{\Delta l}$ [V]	Δl [mm]	0.1050	0.0075	0.9998		Figure 13b
	500:1	unloading	$U_{\Delta l}$ [V]	Δl [mm]	0.1049	−0.0010	1.0000	from	Figure 13b

9. Cyclic Load Tests

Verification of the functionality of the upgraded and digitized measurement chain based on the FPZ 100/1 machine, its calibrated transducers TD1 and TD2 and the suitability of its use in fatigue analyses was carried out in low-cycle fatigue tests. In total, a set of four long-term experimental measurements was carried out. Sets of two measurements were made using the TD1 transducer and sets of a further measurements were made using the TD2 transducer. The recording of these tests was carried out using the electrical signal output of the FPZ 100/1 test machine according to the same electrical wiring diagram, i.e., using the SCM module, MF 624 I/O card and PC assembly (Figure 3), as for the calibration of TD1 and TD2. In all cases, the lower value of the load or load force and therefore its corresponding value of the normal stress was set to zero. Thus, this was a tensile (positive) vanishing cyclic load. One of the reasons for the choice of such a mode was that the test machine, by virtue of its configuration, does not allow cyclic loading simultaneously with different orientation or sign of the load. At the same time, it was inherently a soft loading, i.e., one that is less preferred in the area of low-cycle fatigue. Test specimens with a circular cross-section with a real diameter of 7.75 mm, with a gauge base length of 50 mm, made of steel 12 010 and 14 109.3 (according to EN STN) with an estimated yield strength of 318 and 317 MPa, respectively, were tested. The cycle period was set to 30 s, corresponding to a frequency of approximately 0.033 Hz. The value of the Scale Factor FS was most often chosen at 40:1 or 500:1.

9.1. Experimental Measurements TD1a

For the planned low-cycle fatigue measurements, it was necessary to ensure that the maximum load values exceeded the yield strength of the material used. The tensile diagram of steel 12 010 (Figure 4a) shows a significant yield strength at the loading force level of 15 kN with a corresponding normal stress level of 318 MPa that had to be overcome. For this test, the loading parameters were set with a lower (minimum) force limit of F_{min} = 0 kN and

an upper (maximum) force limit of F_{max} = 17 kN (in Figure 4a as F_{TD1a}) and σ_{max} = 360 MPa, respectively. This stress value for the positively vanishing load also corresponded to the normal stress range $\Delta\sigma$. The Scaling Factor SF was set to 40:1. The specified number of cycles was N = 500. The test was terminated after the specified number of cycles. The values obtained were recorded in two files, the first for force and the second for strain.

The situation for the analysis of test specimen 12 010 under cyclic loading with the application of transducer TD1 in both TD1a and TD1b mode is shown in Figure 14.

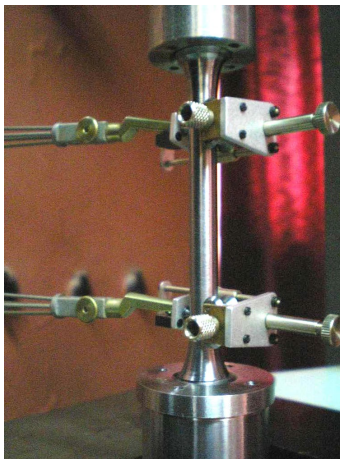

Figure 14. Situation during the analysis of the test specimen of material 12 010 under cyclic loading with the application of transducer TD1 in TD1a and TD1b mode.

Subsequently, the obtained signal attributed to the deformation was transformed to real strain values using the transformation dependence calibration curve according to Figure 12. Thus, the time dependence of the strain ε obtained for the TD1a measurement is shown in Figure 15.

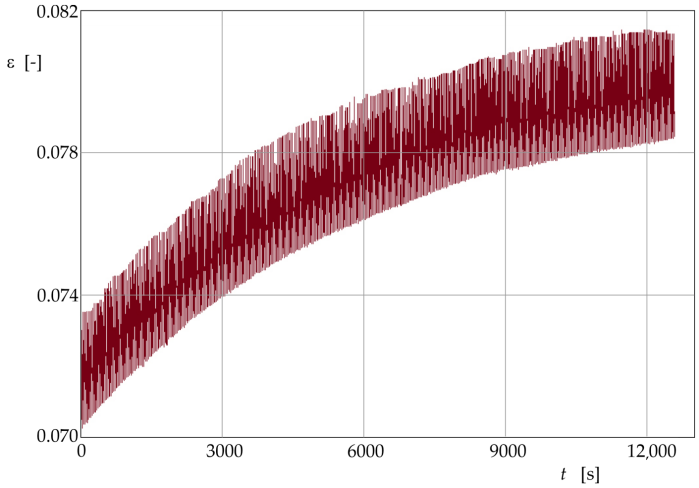

Figure 15. Time dependence of the relative deformation ε when measuring TD1a with the parameters: transducer TD1, Specimen No. 2, F = 0–17 kN, N = 500, and Scale Factor SF = 40:1.

The construction of the normal stress vs. strain dependence, i.e., also of the possible hysteresis loops, should be carried out only for certain cycles for better illustration. Standards on fatigue testing methodologies for metallic materials from all cycles recommend the use of selected cycles, preferably $1{\cdot}10^n$, $2{\cdot}10^n$ and $5{\cdot}10^n$ for powers of n = 0, 1, 2, 3 and 4. In this case, cycles 1–5, 10, 20, 50, 100, 200 and 500 were used (Figure 16).

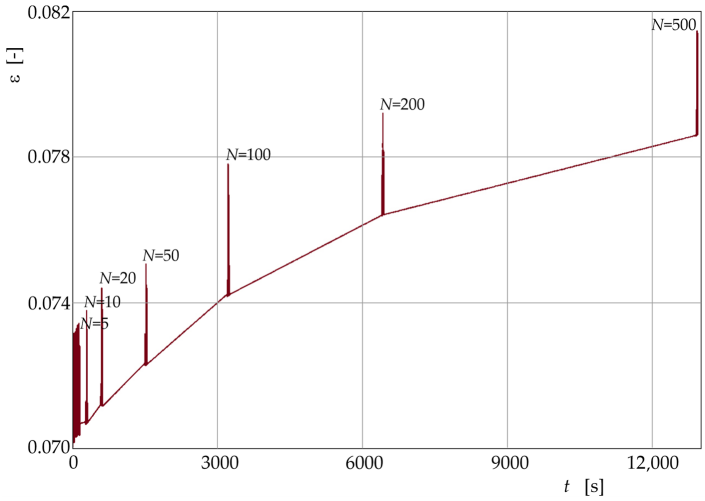

Figure 16. Time dependence of the relative deformation ε for selected cycles for TD1a measurement with parameters: transducer TD1, Specimen No. 2, F = 0–17 kN, N = 1–5, 10, 20, 50, 100, 200 and 500, and Scale Factor SF = 40:1.

Similarly, these cycles were also selected from the total load time course. By comparing these values with the values attributed to the strain, the desired normal stress vs. strain relationship was constructed according to Figure 17. Considering the nature, distribution and clear formation of the hysteresis loops, it is possible to infer a gradual strain hardening of the material.

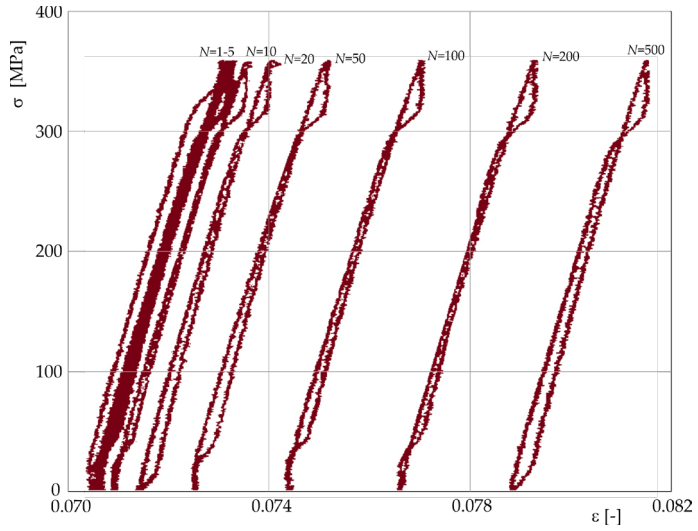

Figure 17. Dependence of the normal stress σ on the strain ε for selected cycles when measuring TD1a with parameters: transducer TD1, Specimen No. 2, F = 0–17 kN, N = 1–5, 10, 20, 50, 100, 200 and 500, and Scale Factor SF = 40:1.

9.2. Experimental Measurements TD1b

Experimental measurements of TD1b were carried out with a similar methodology as for TD1a. Also, in this case, it was necessary to overcome the yield strength level for the material 12 010 in the experiment. For this test, the loading parameters were set with a lower (minimum) force limit of F_{min} = 0 kN and an upper (maximum) force limit of F_{max} = 20 kN (in Figure 4a as F_{TD1b}) and σ_{max} = 424 MPa, respectively. This stress value for the positively vanishing load also corresponded to the normal stress range Δσ. The Scale Factor SF was set to 40:1. The specified number of cycles was initially N = 500. However, the test was terminated after 78 cycles because the strain started to increase rapidly. This

increase was associated with the development of a local constriction (neck) on the test specimen. The values obtained were recorded in two sets, the first for strength and the second for strain.

The data were processed in the same way as in the previous case. That is, the obtained signal attributed to the deformation was transformed to real strain values using the transformation dependence calibration curve according to Figure 12. In this way, the time dependence of the strain ε for the TD1b measurement was obtained is shown in Figure 18.

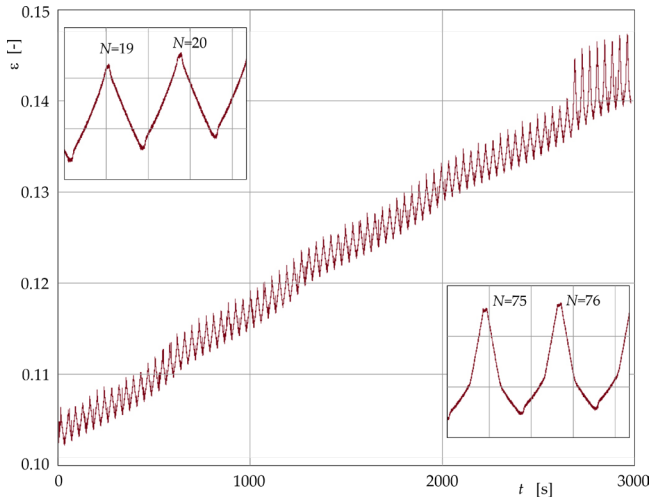

Figure 18. Time dependence of the strain ε for TD1b measurement with the parameters: transducer TD1, Specimen No. 2, F = 0–20 kN, N = 78, and Scale Factor SF = 40:1.

To construct the normal stress vs. strain relationship, i.e., also possible hysteresis loops, cycles of 1–5, 10, 20, 50, 70 and 78 were used according to Figure 19.

This dependence shows that under soft loading in the area of large plastic deformation, the material softens, i.e., the plastic strain grows, determined by the width of the hysteresis loop, increases.

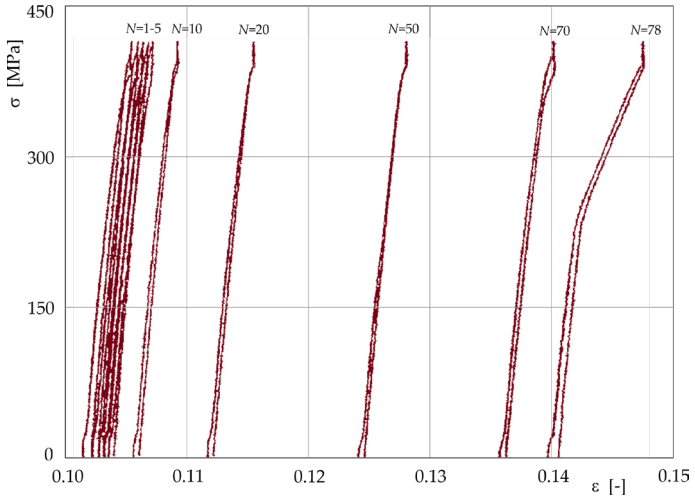

Figure 19. Dependence of the normal stress σ on the strain ε for selected cycles for TD1b measurements with parameters: transducer TD1, Specimen No. 2, F = 0–20 kN, N = 1–5, 10, 20, 50, 70 and 78, and Scale Factor SF = 40:1.

9.3. Experimental Measurements TD2a

Experimental measurements of TD2 were performed with a similar methodology as for TD1. In this case, the experimental yield strength level also had to be overcome, but

for material 14 109.3. However, this showed approximately the same yield strength as for 12 010, namely 317 MPa, according to Figure 4b. For this test, the loading parameters were set with a lower (minimum) force limit of F_{min} = 0 kN and an upper (maximum) force limit of F_{max} = 17 kN (in Figure 4b as F_{TD2a}) and σ_{max} = 360 MPa, respectively. This stress value for the positively vanishing load also corresponded to the normal stress range $\Delta\sigma$. The Scale Factor SF was set to 500:1. The specified number of cycles was set to N = 100. The values obtained were recorded in two files, the first for force and the second for strain.

The data were processed in the same way as in the previous case. The obtained signal attributed to the deformation was transformed to real strain values using the transformation dependence calibration curve according to Figure 13b. In this way, the time dependence of the strain ε for the TD2a measurement was obtained according to Figure 20. This relationship shows that the material has been strain hardened at the test interval.

To construct the normal stress vs. strain relationship, i.e., also possible hysteresis loops, cycles of 1–5, 10, 20, 50 and 100 were used according to Figure 21.

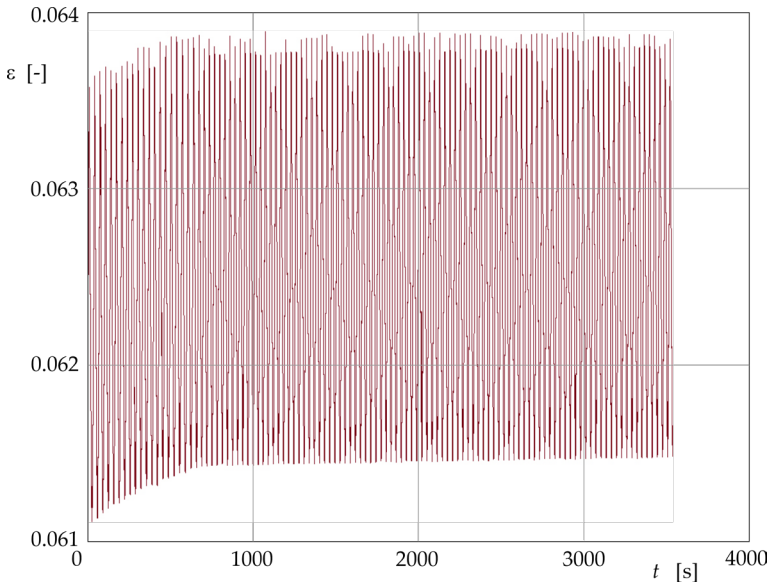

Figure 20. Time dependence of the strain ε when measuring TD2a with the parameters: transducer TD2, Specimen No. 4, F = 0–17 kN, N = 100, and Scale Factor SF = 500:1.

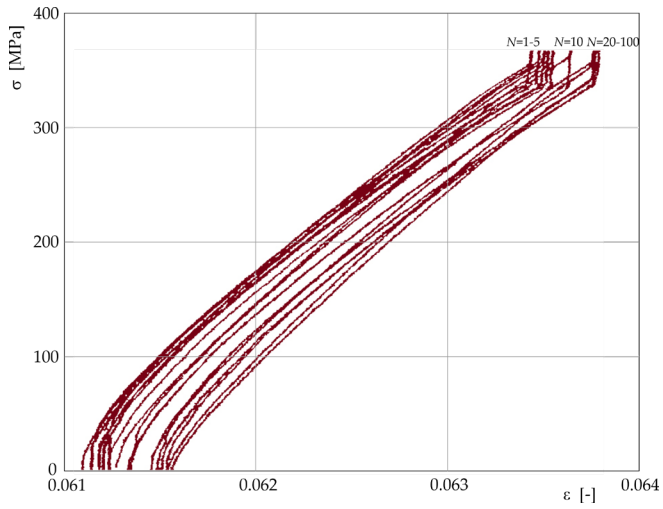

Figure 21. Dependence of the normal stress σ on the strain ε for selected cycles when measuring TD2a with the parameters: transducer TD2, Specimen No. 4, F = 0–17 kN, N = 1–5, 10, 20, 50 and 100, and Scale Factor SF = 500:1.

9.4. Experimental Measurements TD2b

In this test, the loading parameters were set with a lower (minimum) force limit of F_{min} = 0 kN and an upper (maximum) force limit of F_{max} = 16 kN (in Figure 4b as F_{TD2b}), and σ_{max} = 339 MPa, respectively. This stress value for the positively vanishing load also corresponded to the normal stress range $\Delta\sigma$. The Scale Factor SF was set to 500:1. The specified number of cycles was set to N = 400. The values obtained were recorded in two files, the first for force and the second for strain.

The data were processed in the same way as in the previous case. The obtained signal attributed to the deformation was transformed to strain values using the transformation dependence calibration curve according to Figure 13b. In this way, the time dependence of the strain ε for the TD2b measurement was obtained according to Figure 22.

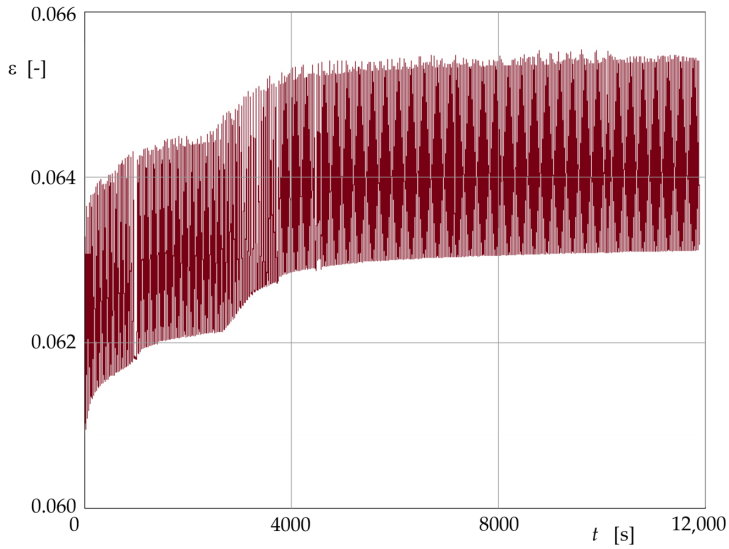

Figure 22. Time dependence of the relative deformation ε for TD2b measurement with parameters: transducer TD2, Specimen No. 4, F = 0–16 kN, N = 400, and Scale Factor SF = 500:1.

To construct the normal stress vs. strain relationship, i.e., also possible hysteresis loops, cycles of 1–5, 10, 20, 50, 100, 200, and 360 were used according to Figure 23.

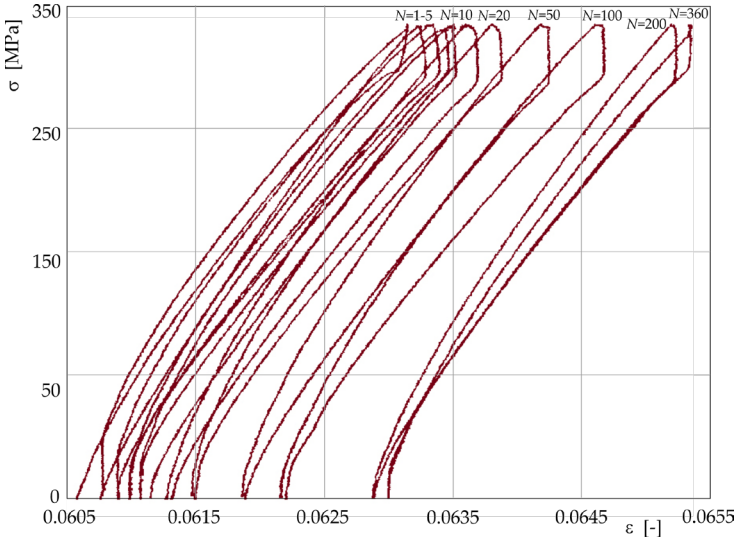

Figure 23. Dependence of the normal stress σ on the strain ε for selected cycles for TD2b measurements with parameters: transducer TD2, Specimen No. 4, F = 0–16 kN, N = 1–5, 10, 20, 50, 100, 200 and 400, and Scale Factor SF = 500:1.

As can be seen from the obtained dependences, during cyclic loading in the first stage (up to about 130 cycles or time 4000 s) there is an alternating strain hardening and softening of the material. At cycle numbers above 150 cycles, it is already possible to observe a strain hardening of the material.

In Table 2, the main parameters of the fatigue tests performed are listed for recapitulation, with the following meaning of each parameter:

Table 2. Parameters of fatigue tests performed.

TD (me.)	Steel No.	σ_y [MPa]	l_0 [mm]	Φd [mm]	T [s]	f [Hz]	F_{min} [kN]	σ_{min} [MPa]	F_{max} [kN]	σ_{max} [MPa]	N [-]	SF [-]	t_{total} [s; min.]	Figure No.
TD1a	12 010	318	50	7.75	30	0.033	0	0	17	360	500	40:1	15,000; 250	Figures 15–17
TD1b	12 010	318	50	7.75	30	0.033	0	0	20	424	78	40:1	2340; 39	Figures 18 and 19
TD2a	14 109.3	317	50	7.75	30	0.033	0	0	17	360	100	500:1	3000; 50	Figures 20 and 21
TD2b	14 109.3	317	50	7.75	30	0.033	0	0	16	339	400	500:1	12,000; 200	Figures 22 and 23

TD (me.)—transducer (measurement), Steel No.—steel modification, σ_y—yield strength, l_0—measurement (gage) length of the specimen, d—diameter of the specimen, T—period, f—frequency, F_{min}—minimum loading force, σ_{min}—minimum loading stress, F_{max}—maximum loading force, σ_{max}—maximum loading stress, N—number of cycles, SF—scale factor, and t_{total}—total measurement time.

10. Summary Evaluation of the Processes Performed and Results

10.1. Evaluation of Measurement Chain Completion Processes

The proposed modifications also included interconnection of the electrical analogue outputs of the FPZ 100/1 device with its transducers TD1 and TD2, calibration probes LARM MSL30.152 PA with the multifunctional I/O card MF 624 and its A/D converter located or interconnected with a PC unit. For this purpose a Signal Conditioning Module (SCM) was designed, manufactured and tested. On the basis of all the verification measurements and their analyses carried out, it can be stated that the newly designed SCM module and its integration into the system together with the other elements created a completely new and functional PC-based measurement chain.

10.2. Evaluation of Calibration Processes and Regression Analyses

The integration and functional verification of the extension sensors-extensometers as TD1 and TD2 transducers based on inductive sensors in two different sensitivity levels from the extensive accessories of the FPZ 100/1 required several processes. These were mainly related to their calibration and to the creation of transformation dependencies between the search quantities elongation Δl and load force F as mechanical quantities and their electrical equivalents in the form of electrical voltage signals $U_{\Delta l}$ and U_F. In addition, single-purpose jigs with integrated industrially produced displacement transducers LARM MSL30.152 PA were designed and manufactured for this purpose.

In some cases of the specimen-material combination, adjustments were made for calibration purposes to extend the elastic deformation region up to several times the original level. This was achieved by a combination of several procedures. In the first phase, this was firstly by strain hardening by previous plastic deformation. As this solution was not sufficiently effective, subsequent heat treatment of the specimens by hardening and tempering was applied.

The reliability and validity of the calibration and transformation dependencies were subsequently assessed by regression and simple correlation analyses. The results of the regression analyses confirmed that the selected linear regression models fully represent the calibration dependencies, with the R^2 determination value not falling below 0.9970. At the same time, the possibility of hysteresis with hysteresis loops formed by the loading and unloading branches of the process was investigated. The obtained results do not indicate

any hysteresis. The exception is the regime $F_{FPZ} = f(U_F)$, which showed a weak hysteresis at a very low level.

The obtained calibration and transformation dependencies were subsequently used in the evaluation of validation experimental measurements of low-cycle fatigue.

10.3. Evaluation of Experimental Low-Cycle Fatigue Tests

The newly obtained modified experimental chain was further verified in terms of the functionality of the modifications made and subsequently the possibility of test measurements in the area of low-cycle fatigue. Several test specimens made of two different steels in several structural states were subjected to the calibration and verification processes of low-cycle high strain fatigue measurements.

From the obtained time dependences of the strain ε and normal stress σ on the strain ε in the form of hysteresis loops for the individual measurement modes TD1a, TD1b, TD2a and TD2b, the behavior of the individual materials in the high strain fatigue range was clearly discernible. These were the expected tendencies of material behavior in terms of the gradual growth of plastic strain, determined by the sizes of the hysteresis loop areas and hence the magnitudes of the dissipated energy, and also in terms of alternating cyclic strain softening and hardening, respectively, and in terms of the gradual global strain hardening of the material. Furthermore, the results obtained also indicated that for tests with cyclic tensile vanishing or pulsating loads, the use of the TD1 version of the transducer appeared to be preferable.

Based on the above experimental measurements and their evaluation, the upgraded functionality of the newly developed measurement chain can be concluded.

10.4. Limitations of the Newly Established Measurement Chain after the Upgrade

However, the newly developed functionality is limited by several factors, e.g., the limited capabilities and modes of the variable load character. These constraints mostly arise from the nature of the basic engineering and design of the upgraded test machine. In this particular case, the machine could operate in either tension-only or compression-only mode, i.e., without the ability to change the sign of the stress during a single-load cycle. This therefore means that it is not possible to carry out a measurement with an alternating symmetrical or alternating asymmetrical cycle. Another technical limitation was related to the possibility of loading rather only in soft loading mode, i.e., with a controlled total load value. This mode is less suitable for low-cycle fatigue measurements, for which measurements in the hard loading mode, i.e., with a controlled specific or total strain value, are more preferred. These factors were also determined by the mode of actuation, which in this case was not preferred electrohydraulic but only electromechanical. One of the other limiting design factors is the relatively low maximum switching frequency at the level of only 0.1 Hz, which cannot be increased without a fundamental redesign of the device.

10.5. Overall Evaluation of the FZP 100/1 Upgrade

By means of the presented modifications, upgrades and digitalization, this example presents a demonstration of the possibility of reincarnation and extension of the moral life of possibly other, newer but also older equipment and their adaptation to the current needs of material testing based on experimental stress and strain analysis, with computer-aided experimentation. These systems, many times still with control, management and registration of results on an analogue basis after digitization, allow the measured data to be further exported and processed in other or third-party analysis programs. At the same time, it was a demonstration of the possibilities of how, on the basis of simple modifications, an existing device can be transformed into a functionally and time-limited operation mode, but at the same time in a mode that was perhaps not foreseen by the manufacturer of the device itself.

10.6. Considerations for Further Upgrade of the FZP 100/1

Considerations for further possible upgrading of the device could also be directed to its modification for measurements not only in the tension–pressure mode but also in a limited mode for the purpose of cyclic loading of specimens during their torsion or even bending.

11. Conclusions

The subject of this paper was the upgrade and modernization of the already existing older universal test equipment HECKERT FPZ 100/1. The aim of the designed, implemented and functionally verified upgrade was the partial digitalization of its exclusively analogue functions of the control, indication and recording processes of sensed and measured data and their analogue outputs. The proposed and implemented procedures were used to investigate the possibility of modifying equipment preferably designed for tensile or compression tests to also perform fatigue tests under simple cyclic tensile–compressive loading.

Some limitations, mainly of a technical nature, were already known before the start of the preparation of the upgrade of the equipment and these limit certain upgrade methods. It is evident that the design and implementation of all modifications to any legacy test equipment will always involve some compromise, tied to the consideration of all major factors, mainly of a technical and economic nature, and taking into account any necessary trade-offs that may arise, with respect to the resulting level and type of functionality and the parameters achieved by the equipment so upgraded.

In this case, however, a measurement chain linking a universal testing machine and a vibration pulsator with a partially digital interface and data acquisition with the ability to perform fatigue tests in a limited mode has been developed at relatively low cost. With this characteristic, this activity can be described as an interim solution and replacement of the orders of magnitude more expensive commercially available systems of today preferably for education purposes or less demanding research purposes or tasks for engineering practice.

Author Contributions: R.H., project administration and supervision; P.S., conceptualization, project administration and writing; I.D., draft preparation, computation and visualization; J.B., methodology and validation; J.V.J., computation and visualization; D.H., computation and visualization. All authors have read and agreed to the published version of the manuscript.

Funding: This work was supported by the Slovak Research and Development Agency under the grant project VEGA No. 1/0152/24, VEGA No. 1/0342/24 and VEGA No. 1/0201/21.

Institutional Review Board Statement: Not applicable.

Informed Consent Statement: Not applicable.

Data Availability Statement: The original contributions presented in the study are included in the article, further inquiries can be directed to the corresponding author.

Conflicts of Interest: The authors declare no conflict of interest.

References

1. Sivák, P.; Delyová, I. *Research of Plasticity and Creep in Selected Stress Conditions of Structural Elements and Materials*, 1st ed.; Kudláček: Jaroměř, Czech Republic, 2023; pp. 117–122.
2. Trebuňa, F.; Šimčák, F. *Limit States—Fractures*, 1st ed.; ManaCon: Prešov, Slovak, 2002; pp. 111–308, (Original in Slovak).
3. Trebuňa, F.; Šimčák, F. *Resistance of Elements of Mechanical Systems*, 1st ed.; Emilena: Košice, Slovak, 2004; pp. 15–968.
4. McAlorum, J.; Rubert, T.; Fusiek, G.; Niewczas, P.; Zorzi, G. Design and demonstration of a low-cost small-scale fatigue testing machine for multi-purpose testing of materials, sensors and structures. *Machines* **2018**, *6*, 30. [CrossRef]
5. Vincent, M.K.; Varghese, V.; Sukumaran, S. Fabrication and analysis of fatigue testing machine. *Int. J. Eng. Sci.* **2016**, *5*, 15–19.
6. Jimenez, G. *Fatigue Testing Machine Redesign and Automation*; Our Knowledge Publishing: Maharashtra, India, 2021.
7. Nozaki, M.; Sakane, M.; Fujiwara, M. Low cycle fatigue testing using miniature specimens. *Int. J. Fatigue* **2020**, *137*, 105636. [CrossRef]
8. Boronski, D. Testing low-cycle material properties with micro-specimens. *Mater. Test.* **2015**, *57*, 165–170. [CrossRef]
9. Shin, C.S.; Lin, S.W. Evaluating fatigue crack propagation properties using miniature specimens. *Int. J. Fatigue* **2012**, *43*, 105–110. [CrossRef]

10. Pach, E.; Korin, I.; Ipina, J.P. Simple fatigue testing machine for fiber-reinforced polymer composite. *Exp. Tech.* **2012**, *36*, 76–82. [CrossRef]
11. Pančík, J.; Beneš, V. IoT challenge: Older test machines modernization in an automotive plant. In *Smart Technology Trends in Industrial and Business Management*; Springer: Berlin/Heidelberg, Germany, 2019; pp. 85–100.
12. Sepahpour, B. A practical educational fatigue testing machine. In Proceedings of the 2014 ASEE Annual Conference & Exposition, Indianapolis, IN, USA, 15–18 June 2014; pp. 24.90.1–24.90.29.
13. Falco, M. Design, Testing, and Analysis of a Novel Fatigue Testing Apparatus. Master's Thesis, University of Rhode Island, Kingston, RI, USA, 2011.
14. Ogawa, F.; Shimizu, Y.; Bressan, S.; Morishita, T.; Itoh, T. Bending and torsion fatigue-testing machine developed for multiaxial non-proportional loading. *Metals* **2019**, *9*, 1115. [CrossRef]
15. Doubrava, K.; Hendrych, S.; Ružička, M. Computer control of FPZ 100 testing machine and its application for basic material tests. In Proceedings of the Esperimental Stress Analysis 39th International Conference, Tábor, Czech Republic, 4–6 June 2001.
16. Gbasouzor, A.I.; Okeke, O.C.; Chima, L.O. Design and characterization of a fatigue testing machine. In Proceedings of the World Congress on Engineering and Computer Science (Vol 1), San Francisco, CA, USA, 23–25 October 2013; pp. 23–25.
17. Wang, D.; Jia, X.; Zhang, D.; Wang, S. A fretting fatigue tester for steel wires and its measuring system. In Proceedings of the International Conference on Mechanical Automation and Control Engineering (MACE), Wuhan, China, 26–28 June 2010; pp. 2398–2401.
18. Ling, H.; Cheng, X.; Yaping, W.; Yongjuan, W. An impact fatigue testing machine to investigate the fatigue lifetime of automatic mechanism key components. In Proceedings of the 16th International Conference on Industrial Engineering and Engineering Management, IE&EM '09, Beijing, China, 21–23 October 2009; pp. 1555–1559.
19. Filčík, P. Possibilities of Using the FPZ 100/1 Test Machine for Low-Cycle Fatigue Tests. Master's Thesis, Technical University of Košice, Košice, Slovak, 2007.
20. Measuring Probes. Length Measuring Gauges MSL30 and MSL50. Available online: http://www.en.larm.cz/measuring-probes/ (accessed on 15 October 2023).
21. Frankovský, P.; Sivák, P.; Delyová, I.; Hroncová, D.; Štuller, P. Rectification of gas pipeline bridging with the support of experimental stress analysis and means of regression and correlation analysis. *Appl. Sci.* **2022**, *12*, 10555. [CrossRef]